

Chapter 3

CONFIGURATION PROPOSALS FOR AN OPTIMAL ELECTROMAGNETIC COUPLING IN IDH SYSTEM

3.1 Introduction

Induction Dielectric Heating (IDH) is a mature technique for heating conducting materials (CM) and non-conducting materials (NCM). To reduce process cycle time with repeated quality, a suitable electromagnetic coupling that in turns generates intense heat throughput at very high rates, at well-defined locations and without considering magnetic permeability has been enabled.

When it comes to induction heating, one must keep in mind that ferromagnetic materials loose their magnetic properties above Curie temperature [4], [11], [70], thus good electric conductor condition exist as to be taken into account for a proper work-piece candidate in a IDH system, whereas low conducting materials will require high frequency for the excitation coil in order to get the above advantages. Other way to overcome the poor electromagnetic coupling in low conductive work-pieces is by way of assembling a high melting temperature condition [86], which is due to its high conductivity which heats indirectly the low conductive insert so as to avoid high frequency supportive equipment thus lowering the capital costs.

Despite IDH is a well-established heating method; the fit a favourable IDH scheme realized on empirical rules, relating size, frequency and the skin depth of the work-piece.

In this chapter the mathematical model for steady state IDH process has been developed and its numerical solution using Matlab and finite element method (FEM) has been obtained. It has been devoted to develop analytic parameters, which are intended to be taken as guidance to set optimal IDH configurations for putting together inductor and work-piece to achieve the highest electromagnetic coupling. It should match optimal conditions that are already known for induction heating practitioners [106], [110]. The simplest and existing geometrical coordinates have been used in massive induction heating systems. Which are the cylindrical and the spherical coordinates.

IDH system can be represented as a three phase high frequency electrical transformer, the more intense heat the influence on the idle coil impedance when the secondary loop is assembled, the greater the occurrence of eddy current on CM and displacement current (rate of change of voltage with respect to time) on NCM. Thus, a proposed reflection coefficient and transmission coefficient has been developed, which is the common factor that precedes both secondary resistance and secondary inductance as appearing in the effective impedance formula for an ideal electrical transformer. The larger reflection coefficient, the better is the electromagnetic coupling of the work-piece. To undertake the task, a dimensionless treatment of simplified governing differential equation of the process has been derived. The above approach has been presented for cylindrical systems [28], [106] and spherical systems, by considering boundary values: either a longitudinal or a transverse magnetic flux. In this chapter same treatment also will be given to cylindrical and spherical work-pieces, namely steel and lemon being excited by a travelling wave.

3.2 Impedance Parameters for an IDH System

A lumped parameter model has been represented in a mathematical model of a physical system where field variables have been simplified. The mathematical analysis of an electrical circuit is much simpler than solving the electromagnetic equations for the actual IDH physical system. Thus impedances, as lumped parameters, are electrical equivalent to those electromagnetic fields distributed in an existing inductor or an element of a circuit. Thereby, magnetic strength and current density distributions for a given IDH configuration, the basic impedance parameters such as resistances and inductances have been

stemmed from and then treated in such a way that a reflection coefficient and transmission coefficient has been obtained as a result.

The properties of an electromagnetic wave (direction of propagation, velocity of propagation, wavelength, frequency, attenuation, phase, intrinsic, skin depth etc.) can be determined by examining the solutions to the wave equations that define the electric and magnetic fields of the wave.

The mathematical model has been developed for two cases as follows:

1. Conducting material (CM)
2. Non-conducting material (NCM)

To obtain the mathematical model, Maxwell's equation and Ohm's law have been used. Displacement current is neglected for CM and eddy current is neglected for NCM. Maxwell's equations provide the following system:

$$\nabla \times H = \text{curl}H = J + \frac{\partial D}{\partial t} \quad (3.1)$$

$$\nabla \cdot B = \text{div}B = 0 \quad (3.2)$$

$$\nabla \times E = \text{curl}E = -\frac{\partial B}{\partial t} \quad (3.3)$$

$$\nabla \cdot D = \text{div}D = \sigma \quad (3.4)$$

$$vB = H \quad (3.5)$$

Where

- E = Electric field intensity in V/m
- H = Magnetic field intensity in A/m
- B = Magnetic inductance (flux density) in Wb/m^2
- D = Electric displacement field in C/m^2
- J = Current density in A/m^2
- v = Magnetic reactivity
- σ = Electrical conductivity in $S.m^{-1}$
- μ = Magnetic permeability in H/m

With other co-relationship

$$D = \epsilon E, \text{For non-conducting material (Dielectric)} \quad (3.6)$$

$$B = \mu H, \text{Magnetic inductance} \quad (3.7)$$

$$J = \sigma E, \text{For conducting material (Metal)} \quad (3.8)$$

valid in the whole space. From Ohm's law,

$$J = J_d + J_e + J_D \quad (3.9)$$

Where

$$\begin{aligned} J_d &= \text{Driving current} \\ J_e &= \text{Eddy current} \\ J_D &= \text{Displacement current inside the materials} \end{aligned}$$

$$J = 0 \text{ in the space outside the materials.} \quad (3.10)$$

This work overlooks the function of the accumulative charges, that is $\sigma = 0$. According to the relationship between D , J , E , B and D ,

$$\nabla \times H = J + \frac{\partial D}{\partial t} = \sigma E + \frac{\partial}{\partial t}(\epsilon E) \quad (3.11)$$

The corresponding vector from

$$\nabla \times H = (\sigma + j\omega\epsilon)E \quad (3.12)$$

$$\nabla \times E = -j\omega\mu H \quad (3.13)$$

$$\nabla \cdot E = 0 \quad (3.14)$$

$$\nabla \cdot H = 0 \quad (3.15)$$

$$\nabla \times \nabla \times E = \nabla(\nabla \cdot E) - \nabla^2 E$$

Substituting values from equation 3.13 and equation 3.14

$$-\nabla^2 E = -j\omega\mu(\nabla \times H) \quad (3.16)$$

By substituting equation 3.12, results as

$$\nabla^2 E = j\omega\mu(\sigma + j\omega\epsilon)E \quad (3.17)$$

$$\nabla^2 E = \gamma^2 E \quad (3.18)$$

Where

$$\gamma^2 = j\omega\mu(\sigma + j\omega\epsilon)$$

γ (gamma) is called propagation constant in m^{-1} and has real and imaginary parts,

$$\gamma = \alpha + j\beta \quad (3.19)$$

Where

α = Attenuation constant in neper/m (Np/m)

β = Phase constant in (rad/m)

The attenuation constant defines the rate at which the fields of the wave is attenuated as the wave propagates. An electromagnetic wave propagates in an ideal (lossless) media without attenuation ($\alpha=0$). The phase constant defines the rate at which the phase changes as the wave propagates.

Taking only the x -component of E , variation with respect to z ,

$$\frac{\partial^2 E_x}{\partial t^2} = -\mu_0 \epsilon_0 \omega^2 E_x$$

$$\frac{\partial^2 E_x}{\partial t^2} + \mu_0 \epsilon_0 \omega^2 \bar{E}_x = 0 \quad (3.20)$$

It is a second order differential equation having complete solution

$$E_x = E_{x0} e^{j\omega t} e^{\pm\gamma z} \quad (3.21)$$

$$E_x = E_{x0} e^{-\alpha z} e^{j(\omega t - \beta z)} \quad (3.22)$$

Where

$$-\gamma x = -\alpha x - j\beta x$$

The factor $e^{-\alpha z}$ shows the attenuation of wave. The phase constant β for a lossy dielectric is different from phase constant of a perfect dielectric of same dielectrics constant and permeability, β increases with conductivity. Hence wave length corresponding to given frequency becomes smaller and velocity of propagation is less.

The propagation constant can be obtained from equation 3.2

$$\gamma^2 = j\omega\mu(\sigma + j\omega\epsilon)$$

$$\gamma = j\omega\sqrt{\mu\epsilon}\sqrt{1 - j\left(\frac{\sigma}{\omega\epsilon}\right)} \quad (3.23)$$

γ can be separated into α and β such that

$$\gamma^2 = (\alpha + j\beta)^2 = j\omega\mu(\sigma + j\omega\epsilon) \quad (3.24)$$

$$\alpha^2 - \beta^2 = -\omega^2\mu\epsilon \quad (3.25)$$

$$2\alpha\beta = \omega\mu\epsilon \quad (3.26)$$

From equation 3.25 and equation 3.26, separate α and β

$$\alpha = \omega \sqrt{\frac{\mu\epsilon}{2} \left(\left[\sqrt{1 + \left(\frac{\sigma}{\omega\epsilon}\right)^2} - 1 \right] \right)} \quad (3.27)$$

$$\beta = \omega \sqrt{\frac{\mu\epsilon}{2} \left(\left[\sqrt{1 + \left(\frac{\sigma}{\omega\epsilon}\right)^2} + 1 \right] \right)} \quad (3.28)$$

Considering only E_x component to E varying w.r.t z

$$\begin{aligned} \nabla X E &= \frac{\partial E_x}{\partial z} 1_y \\ &= 1_y \frac{\partial}{\partial z} E_{x0} e^{-\gamma z} \\ &= -1_y \gamma E_{x0} e^{-\gamma z} \end{aligned}$$

Substituting equation 3.13

$$-j\omega\mu H = -1_y \gamma E_{x0} e^{-\gamma z}$$

H has H_y component corresponding to E_x

$$H_y = \frac{\gamma}{j\omega\mu} E_x \quad (3.29)$$

So the intrinsic impedance

$$\eta = \frac{E_x}{H_y} = \frac{j\omega\mu}{\gamma} \quad (3.30)$$

Substituting γ from equation 3.23

$$\eta = \sqrt{\frac{\mu}{\epsilon \left(1 + j \frac{\sigma}{j\omega\epsilon} \right)}} = \sqrt{\frac{j\omega\mu}{\sigma + j\omega\epsilon}} \quad (3.31)$$

η is a complex quantity

$$\eta = \eta_m \angle \theta_\eta \quad (3.32)$$

With

$$E_x = E_{x0} e^{-\alpha z} e^{j(\omega t - \beta z)} \quad (3.33)$$

$$= E_{x0} e^{-\alpha z} (\cos(\omega t - \beta z) + j \sin(\omega t - \beta z)) \quad (3.34)$$

The magnetic field intensity becomes

$$\begin{aligned}
 H_y &= \frac{E_{x0}}{\eta} e^{-\alpha z} e^{j(\omega t - \beta z)} \\
 &= \frac{E_{x0}}{\eta} e^{-\alpha z} (\cos(\omega t - \beta z) + j \sin(\omega t - \beta z)) \\
 &= \frac{E_{x0}}{\eta_m} e^{-\alpha z} (\cos(\omega t - \beta z - \theta_\eta) + j \sin(\omega t - \beta z - \theta_\eta))
 \end{aligned} \tag{3.35}$$

The electric and magnetic fields is no longer in time phase.

The factor $e^{-\alpha z}$ causes an exponential decrease in amplitude with increasing values of z ; η is a complex quantity in the first quadrant, so the electric field leads the magnetic field in time phase.

Since P is given by the cross product of E and H , the direction of power flow at any point is normal to both the E and H vectors. This certainly agrees with our experience with the uniform plane wave, for propagation in the $+z$ direction was associated with an E_x and H_y component,

$$E_x a_x \times H_y a_y = P_z a_z \tag{3.36}$$

Thus,

$$\begin{aligned}
 P_z &= E_x H_y \\
 &= \frac{E_{x0}^2}{\eta_m} e^{-2\alpha z} (\cos(\omega t - \beta z) + j \sin(\omega t - \beta z)) \\
 &\quad (\cos(\omega t - \beta z - \theta_\eta) + j \sin(\omega t - \beta z - \theta_\eta)) \\
 &= \frac{1}{2} \frac{E_{x0}^2}{\eta_m} e^{-2\alpha z} [\cos(2\omega t - 2\beta z - 2\theta_\eta) + \cos\theta_\eta]
 \end{aligned} \tag{3.37}$$

From equation 3.37, it can be seen that the power density has only a second harmonic component and a DC component. Since the first term has zero average value over an integral number of periods, the time average value of the Poynting vector

$$P_{z,av} = \frac{1}{2} \frac{E_{x0}^2}{\eta_m} e^{-2\alpha z} [\cos(2\omega t - 2\beta z - 2\theta_\eta) + \cos\theta_\eta] \tag{3.38}$$

Note that the power density attenuates as $e^{-2\alpha z}$, where as E_x and H_y fall off as $e^{-\alpha z}$

The dividing line between two classes is not sharp and some media has considered as conducting material (conductors) in one part of high frequency range, but as non-conducting material (dielectric) (with loss) in another part of the range.

In the Maxwell's equation $\nabla \times H = \sigma E + j\omega \epsilon E$, the ratio $\frac{\sigma}{\omega \epsilon}$ is therefore just the ratio of conduction current density to displacement current density in the medium. Conducting material has $\frac{\sigma}{\omega \epsilon} \gg 1$ over entire high frequency range. Non-conducting material has $\frac{\sigma}{\omega \epsilon} \ll 1$ under the high frequency range.

The term $\frac{\sigma}{\omega \epsilon}$ is referred to as the loss tangent (similar to loss tangent in case of a capacitor) or dissipation factor. In practice, following observations are true:

1. For good conductors σ and ω are nearly independent of frequency.
2. For most dielectrics σ and ω are functions of frequency, but the ratio $\frac{\sigma}{\omega \epsilon}$ is often constant over the frequency range of interest.

Based on the value of $\frac{\sigma}{\omega \epsilon}$, it can be approximate the relations for attenuation constant, phase constant and intrinsic impedance for CM and NCM.

3.3 Conducting Material

For the development of mathematical model for conducting material following assumptions have been made,

1. All CM are cylindrical, magnetic and have no net electric charge.
2. The system is rotationally symmetric about the z-axis i.e. θ for conducting material e.g. steel.
3. The rate of change of output voltage with respect to time is neglected for conducting material (CM).
4. The distribution of electrical current and travelling magnetic flux in the coil is uniform.
5. The self inductance effect in the coil is taken into account.
6. The current has a steady state quality and as a result, the electromagnetic field quantities are harmonically oscillating functions with a fixed single frequency.

3.3.1 Wave propagation in conducting material (CM)

For conducting material $\sigma \gg \omega\epsilon$

$$\frac{\sigma}{\omega\epsilon} \gg 1 \quad (3.39)$$

The propagation constant γ can be written as

$$\begin{aligned} \gamma^2 &= j\omega\mu(\sigma + j\omega\epsilon) \\ &= j\omega\mu\sigma \left(1 + j\frac{\omega\epsilon}{\sigma}\right) \\ &\approx j\omega\mu\sigma \\ \gamma &= \sqrt{j\omega\mu\sigma} \\ &= \sqrt{\omega\mu\sigma} \angle 45^\circ \\ &= \sqrt{\omega\mu\sigma}(\cos 45^\circ + j\sin 45^\circ) \end{aligned} \quad (3.40)$$

$$\begin{aligned} &= \sqrt{\frac{\omega\mu\sigma}{2}} + j\sqrt{\frac{\omega\mu\sigma}{2}} \\ &= (1 + j)\sqrt{\frac{\omega\mu\sigma}{2}} \end{aligned} \quad (3.41)$$

$$\text{So } \alpha = \beta = \sqrt{\frac{\omega\mu\sigma}{2}} = \sqrt{\pi f\mu\sigma} \quad (3.42)$$

The velocity of propagation

$$\nu = \frac{\omega}{\beta} = \sqrt{\frac{2\omega}{\mu\sigma}} \quad (3.43)$$

The intrinsic impedance of the CM

$$\eta = \sqrt{\frac{j\omega\mu}{\sigma + j\omega\epsilon}} = \sqrt{\frac{j\omega\mu}{\sigma}} = \sqrt{\frac{\omega\mu}{\sigma}} \angle 45^\circ \quad (3.44)$$

In a conductor, α and β are large. The wave attenuates greatly as it progresses and phase shift per unit length is also large. The velocity of the wave is small. The intrinsic impedance is small and has a reactive component with impedance angle of 45° .

3.3.2 Mathematical model for CM (Steel)

Let (a_r, a_θ, a_z) be the natural tangent system associated with cylindrical coordinate, (r, θ, z) such that the O_z -axis is the symmetry axis of the induction dielectric heating



Where

σ_{co} = The electrical conductivity of the coil

σ_w = The electrical conductivity of the work-piece

Setting $J_d = J_0 \cos \omega t$ as the driving current in the coil, to find a solution of the from

$$\begin{aligned} \nabla X \left(\left(\frac{J_e}{\sigma_{co}} + j\omega\psi \right) a_\theta \right) &= 0, \text{For coil} \\ \nabla X \left(\left(\frac{J_e}{\sigma_w} + j\omega\psi \right) a_\theta \right) &= 0, \text{For work-piece} \end{aligned} \quad (3.52)$$

It follows that for coil $\left(\frac{J_e}{\sigma_{co}} r + j\omega\psi r \right)$ and for work-piece $\left(\frac{J_e}{\sigma_w} r + j\omega\psi r \right)$ are a constant in each connected components of a conductor and shows that this constant is equal to $v_k/2\pi$.

$$\begin{aligned} J &= \sigma_{co} \left(-j\omega\psi + \frac{v_k}{2\pi r} \right), \text{Coil} \\ J &= \sigma_w \left(-j\omega\psi + \frac{v_k}{2\pi r} \right), \text{Work-piece} \end{aligned} \quad (3.53)$$

Where

v_k = Total voltage imposed in the conductor

Using equation 3.1, equation 3.5, equation 3.48 and equation 3.53, to get inside the conducting materials (coils and work-pieces) the equation

$$\begin{aligned} - \left(\frac{\partial}{\partial r} \left(\frac{v}{r} \frac{\partial r \psi}{\partial r} \right) + \frac{\partial}{\partial z} \left(v \frac{\partial \psi}{\partial z} \right) \right) + j\sigma_{co}\omega\psi &= \sigma_{co} \frac{v_k}{2\pi r}, \text{Coil} \\ - \left(\frac{\partial}{\partial r} \left(\frac{v}{r} \frac{\partial r \psi}{\partial r} \right) + \frac{\partial}{\partial z} \left(v \frac{\partial \psi}{\partial z} \right) \right) + j\sigma_w\omega\psi &= \sigma_w \frac{v_k}{2\pi r}, \text{Work-piece} \end{aligned} \quad (3.54)$$

In a similar way the relation from equation 3.1, equation 3.5, equation 3.10 and equation 3.48 are combined together will provide the following equation in the space outside the conductors.

$$\left(\frac{\partial}{\partial r} \left(\frac{v}{r} \frac{\partial r \psi}{\partial r} \right) + \frac{\partial}{\partial z} \left(v \frac{\partial \psi}{\partial z} \right) \right) = 0 \quad (3.55)$$

Since there are no surface current, the following interface condition holds at the boundary of any conductor

$$\left[\frac{v}{r} \left(\frac{\partial(r\psi)}{\partial r} n_r + \frac{\partial(r\psi)}{\partial z} n_z \right) \right] = 0 \quad (3.56)$$

Where $[\psi]$ denotes the jump of a function ψ at the boundary of the conducting material and $n = n_r a_r + n_z a_z$ is the normal vector on the interface.

For electromagnetic computations, consider a circular in the (r, z) -plan, surrounding the induction dielectric heating system and big enough for the magnetic field to be weak at the boundaries of the outer surface.

The Bio-Savart hypothesis implies that the field B behave like $1/(r^3 + z^3)$ far from the conductors. For big values of r , the behaviour of ψ can be considered to be similar to $1/r^2$. Therefore, on the boundaries of the outer surface which are parallel to the symmetry axis, so called Robin condition [[55] p.162].

$$\frac{\partial(r\psi)}{\partial r} + \psi = 0 \quad (3.57)$$

For those boundaries of the outer surface which are perpendicular to the symmetry axis, a Robin like condition is difficult to enforce. Instead, the condition.

$$\frac{\partial(r\psi)}{\partial z} = 0 \quad (3.58)$$

Which stems from the assumptions that the radial component of the magnetic field is close to zero on these boundaries.

Finally, the natural symmetry condition along the revolution axis is

$$\psi = 0 \quad (3.59)$$

To sum up, the electromagnetic model to be solved consists of equation 3.53 and equation 3.54, together with the interface condition equation 3.55, the boundary conditions equation 3.58 and equation 3.57, as well as the symmetry condition equation 3.59.

In order to study the thermal effects of the electromagnetic phenomena, the above model will be coupled with the heat equation. Assume that the work-pieces do not interact thermally. These assumptions will allow solving the heat equation individually for each work-piece. The Joule effect power term is $\sigma^{-1}|J_m|^2$, where J_m is the mean current density, equal to $J/\sqrt{2}$ in our case. The value of J is directly obtained by equation 3.53. Therefore, the equation to be solved in order to get the temperature field in the work-piece is

$$\rho C_p \frac{\partial T}{\partial t} - (\lambda \nabla T) = \frac{\sigma_w}{2} \left| \left(-j\omega\psi + \frac{v_k}{2\pi r} \right) \right|^2 \quad (3.60)$$

Equation 3.60 is completed by the following radiation condition on the boundary of the work-piece, which is justified if the work-piece is convex and there is a large difference in temperature between the work-piece and the surrounding space:

$$\lambda \frac{\partial T}{\partial n} + \kappa(T^4 - T_{amb}^2) = 0 \quad (3.61)$$

Where

- κ = The product of the Stefan Boltzmann constant by the material emissivity coefficient
 $\partial T/\partial n$ = The normal derivative of T on the boundary of the work-piece
 T_{amb} = The ambient temperature

One can also consider an empirical conversion law, replacing equation 3.61 by the condition

$$\lambda \frac{\partial T}{\partial n} + \kappa(T^4 - T_{amb}^4) + \zeta(T - T_{amb}) = 0 \quad (3.62)$$

Where

- ζ = Proportionality coefficient

The complete model consists in coupling the electromagnetic problem equation 3.53-equation 3.59 with the thermal problem equation 3.60, equation 3.61, or equation 3.62, where T depends only on the spatial coordinates r , z and on the time t .

This model includes two kinds of nonlinearities: the first due to the heat source term in the heat equation 3.57 and the second due to the dependence of physical properties of the conducting materials on the temperature and possibly on the magnetic field.

3.4 Non-Conducting Material

For the development of mathematical model for non-conducting material following assumptions have been made,

1. All NCM are isotropic, non-magnetic and have no net electric charge.
2. The system is rotationally symmetric about the z-axis i.e. ϕ for non-conducting material e.g. lemon.
3. The eddy current is neglected for non-conducting material (NCM).
4. The distribution of potential in the coil is uniform.
5. The self capacitance effect in the coil is taken into account.
6. The voltage has a steady state quality and as a result, the electromagnetic field quantities are harmonically oscillating functions with a fixed single frequency.

3.4.1 Wave propagation in non-conducting material (NCM)

For non-conducting material

$$\sigma \ll \omega \epsilon \text{ or}$$

$$\frac{\sigma}{\omega \epsilon} \ll 1$$

It can be written as

$$\sqrt{1 + \frac{\sigma^2}{\omega^2 \epsilon^2}} \approx \left(1 + \frac{\sigma^2}{2\omega^2 \epsilon^2}\right) \quad (3.63)$$

by using binomial theorem

$$(1 + x)^n = 1 + nx + \frac{n(n-1)}{2!}x^2 + \frac{n(n-1)(n-2)}{3!}x^3 + \dots \quad (3.64)$$

Equation 3.27 and equation 3.28 then becomes

$$\begin{aligned} \alpha &= \omega \sqrt{\frac{\mu \epsilon}{2} \left(\sqrt{1 + \left(\frac{\sigma}{\omega \epsilon}\right)^2} - 1 \right)} \\ &\approx \omega \sqrt{\frac{\mu \epsilon}{2} \left(1 + \frac{\sigma^2}{2\omega^2 \epsilon^2} - 1 \right)} \\ &= \frac{\sigma}{2} \sqrt{\frac{\mu}{\epsilon}} \end{aligned} \quad (3.65)$$

$$\begin{aligned} \beta &= \omega \sqrt{\frac{\mu \epsilon}{2} \left(\sqrt{1 + \left(\frac{\sigma}{\omega \epsilon}\right)^2} + 1 \right)} \\ &\approx \omega \sqrt{\frac{\mu \epsilon}{2} \left(1 + \frac{\sigma^2}{2\omega^2 \epsilon^2} + 1 \right)} \\ &= \omega \sqrt{\mu \epsilon} \left(1 + \frac{\sigma^2}{8\omega^2 \epsilon^2} \right) \end{aligned} \quad (3.66)$$

$\omega \sqrt{\mu \epsilon} = \left(\frac{\omega}{v}\right)$ is the phase shift for a non-conducting material.

$$\begin{aligned} \text{Velocity of wave } \nu &= \frac{\omega}{\beta} \\ &= \frac{1}{\sqrt{\mu \epsilon \left(1 + \frac{\sigma^2}{8\omega^2 \epsilon^2} \right)}} \\ &\approx \frac{1}{\sqrt{\mu \epsilon}} \left(1 - \frac{\sigma^2}{8\omega^2 \epsilon^2} \right) \end{aligned} \quad (3.67)$$

$\frac{1}{\sqrt{\mu\varepsilon}}$ is the velocity of the wave in the NCM when the conductivity is zero i.e. in perfect dielectric. The effect of a small amount of loss is to reduce slightly the velocity of propagation of the wave.

$$\begin{aligned} \text{Intrinsic impedance } \eta &= \sqrt{\frac{j\omega\mu}{\sigma + j\omega\varepsilon}} \\ &= \sqrt{\frac{\mu}{\varepsilon} \left(\frac{1}{1 + \frac{\sigma}{j\omega\varepsilon}} \right)} \\ &\approx \sqrt{\frac{\mu}{\varepsilon}} \left(1 + j\frac{\sigma}{2\omega\varepsilon} \right) \end{aligned} \quad (3.68)$$

$\sqrt{\frac{\mu}{\varepsilon}}$ is the intrinsic impedance of the NCM with $\sigma = 0$. The chief effect of loss is to add a small reactive component to the intrinsic impedance.

The above approximations may be made in the cases where $\frac{\sigma}{\omega\varepsilon} < 0.1$.

3.4.2 Mathematical model for NCM (Lemon)

Let (a_r, a_θ, a_ϕ) be the natural tangent system associated with spherical coordinate (r, θ, ϕ) such that the O_θ -axis is the symmetry axis of the induction dielectric heating (IDH). The current density is supposed to be in the form $J = J(r, \theta)e^{j\omega t}a_\phi$, where ω is the angular frequency of the current and t is the time. It is also assumed that the components of the fields H, E, B in the system (a_r, a_θ, a_ϕ) depend only on r, θ and t (not on ϕ). Equation 3.1 yields then that $H(r, \theta)$ is of the form

$$H(r, \theta) = (H_r(r, \theta)a_r + H_\theta(r, \theta)a_\theta)e^{j\omega t} \quad (3.69)$$

Let A be a magnetic vector potential, i.e., a magnetic field satisfying

$$B = \nabla \times A \quad (3.70)$$

A is divergence free (coulomb gauge). Using equation 3.5, equation 3.69 and equation 3.70, it can be shown that A may be expressed in terms of a continuous scalar potential ψ depending only on r and θ :

$$A = e^{j\omega t}\psi(r, \theta)a_\phi \quad (3.71)$$

Using the notation $B(r, \theta) = (B_r(r, \theta)a_r + B_\theta(r, \theta)a_\theta)e^{j\omega t}$, from equation 3.70

$$\begin{aligned} B_r &= \frac{1}{r \sin \theta} \frac{\partial(\psi \sin \theta)}{\partial \theta} \\ B_\theta &= -\frac{1}{r} \frac{\partial r \psi}{\partial r} \end{aligned} \quad (3.72)$$

From equation 3.3

$$\nabla X E + j\omega B = 0 \quad (3.73)$$

and using equation 3.46

$$\nabla X(E + j\omega A) = 0 \quad (3.74)$$

Include the self inductance effect in the induction coil as displacement current represented by $J_D = \partial D / \partial t = j\omega D = j\omega \epsilon E$ as per equation 3.8. The eddy current is neglected for non-conducting material, then

$$\begin{aligned} J &= J_d + J_D = J_d + j\omega \epsilon_{co} E, \text{Driving and displacement current in the coil} \\ &= J_D = j\omega \epsilon_w E, \text{Displacement current in the work-piece} \end{aligned} \quad (3.75)$$

Where

ϵ_{co} = The electrical permittivity of the coil

ϵ_w = The electrical permittivity of the work-piece

Setting $J_d = J_0 \cos \omega t$ as the driving current in the coil, to find a solution of the form

$$\begin{aligned} \nabla X \left(\left(\frac{J_D}{j\omega \epsilon_{co}} + j\omega \psi \right) a_\phi \right) &= 0, \text{For coil} \\ \nabla X \left(\left(\frac{J_D}{j\omega \epsilon_w} + j\omega \psi \right) a_\phi \right) &= 0, \text{For work-piece} \end{aligned} \quad (3.76)$$

It follow that for coil $\left(\frac{J_D}{j\omega \epsilon_w} r + j\omega \psi r \right)$ and for work-piece $\left(\frac{J_D}{j\omega \epsilon_w} r + j\omega \psi r \right)$ are a constant in each connected components of a lemon and shown that this constant is equal to $v_k / 2\pi$.

$$\begin{aligned} J &= j\omega \epsilon_{co} \left(-j\omega \psi + \frac{v_k}{2\pi r} \right), \text{Coil} \\ J &= j\omega \epsilon_w \left(-j\omega \psi + \frac{v_k}{2\pi r} \right), \text{Work-piece} \end{aligned} \quad (3.77)$$

Where

v_k = Total voltage imposed in the lemon (NCM)

Using equation 3.1, equation 3.5, equation 3.72 and equation 3.77, inside the non-conducting materials (coils and work-pieces) the equation

$$\begin{aligned} - \left(\frac{\partial}{\partial r} \left(\frac{v}{r^2 \sin \theta} \frac{\partial r \psi \sin \theta}{\partial r} \right) + \frac{\partial}{\partial \theta} \left(\frac{v}{r} \frac{\partial r \psi}{\partial \theta} \right) \right) - \omega^2 \epsilon_{co} \psi &= j \omega \epsilon_{co} \frac{v_k}{2 \pi r}, \text{Coil} \\ - \left(\frac{\partial}{\partial r} \left(\frac{v}{r^2 \sin \theta} \frac{\partial r \psi \sin \theta}{\partial r} \right) + \frac{\partial}{\partial \theta} \left(\frac{v}{r} \frac{\partial r \psi}{\partial \theta} \right) \right) - \omega^2 \epsilon_w \psi &= j \omega \epsilon_w \frac{v_k}{2 \pi r}, \text{Work-piece} \end{aligned} \quad (3.78)$$

In a similar way the relation from equation 3.1, equation 3.5, equation 3.10 and equation 3.72 are combined together will provide the following equation in the space outside the conductors.

$$\left(\frac{\partial}{\partial r} \left(\frac{v}{r^2 \sin \theta} \frac{\partial (r \psi \sin \theta)}{\partial r} \right) + \frac{\partial}{\partial \theta} \left(\frac{v}{r} \frac{\partial r \psi}{\partial \theta} \right) \right) = 0 \quad (3.79)$$

Since there are no surface current, the following interface condition holds at the boundary of any non-conductor material

$$\left[\frac{v}{r} \left(\frac{1}{r \sin \theta} \frac{\partial (r \psi \sin \theta)}{\partial r} n_r + \frac{\partial (r \psi)}{\partial \theta} n_\theta \right) \right] = 0 \quad (3.80)$$

Where $[\psi]$ denotes the jump of a function ψ at the boundary of the non-conducting material and $n = n_r a_r + n_\theta a_\theta$ is the normal vector on the interface.

For electromagnetic computations, consider a sphere in the (r, θ) -plan, surrounding the IDH system and big enough for the magnetic field to be weak at the boundaries of the outer surface.

The Bio-Savart hypothesis implies that the field B behave like $1/(r^3 + \theta^3)$ far from the lemon. For big values of r , the behaviour of ψ can be considered to be similar to $1/r^2$. Therefore, on the boundaries of the outer surface which are parallel to the symmetry axis, so called Robin condition [[55] p.162].

$$\frac{\partial (r \psi \sin \theta)}{\partial r} + \psi = 0 \quad (3.81)$$

For those boundaries of the outer surface which are perpendicular to the symmetry axis, a Robin like condition is difficult to enforce. Instead, the condition

$$\frac{\partial (r \psi)}{\partial \theta} = 0 \quad (3.82)$$

Which stems from the assumptions that the radial component of the magnetic field is close to zero on these boundaries.

Finally, the natural symmetry condition along the revolution axis is

$$\psi = 0 \quad (3.83)$$

To sum up, the electromagnetic model to be solved consists of equation 3.77 and equation 3.78, together with the interface condition equation 3.79, the boundary conditions equation 3.82 and equation 3.81, as well as the symmetry condition equation 3.83.

In order to study the thermal effects of the electromagnetic phenomena, the above model will be coupled with the heat equation. Assume that the work-pieces do not interact thermally. These assumptions will allow solving the heat equation individually for each work-piece. The Rubbing effect power term is $|J_m|^2/j\omega\epsilon$, where J_m is the mean current density, equal to $J/\sqrt{2}$ in our case. The value of J is directly obtained by equation 3.77. Therefore, the equation to be solved in order to get the temperature field in the work-piece is

$$\rho C_p \frac{\partial T}{\partial t} - (\lambda \nabla T) = \frac{j\omega\epsilon_w}{2} \left| \left(-j\omega\psi + \frac{v_k}{2\pi r} \right) \right|^2 \quad (3.84)$$

Equation 3.84 is completed by the following radiation condition on the boundary of the work-piece, which is justified if the work-piece is convex and there is a large difference in temperature between the work-piece and the surrounding space:

$$\lambda \frac{\partial T}{\partial n} + \kappa(T^4 - T_{amb}^2) = 0 \quad (3.85)$$

Where

- κ = The product of the Stefan Boltzmann constant by the material emissivity coefficient
- $\partial T/\partial n$ = The normal derivative of T on the boundary of the work-piece
- T_{amb} = The ambient temperature

One can also consider an empirical conversion law, replacing equation 3.85 by the condition

$$\lambda \frac{\partial T}{\partial n} + \kappa(T^4 - T_{amb}^4) + \zeta(T - T_{amb}) = 0 \quad (3.86)$$

Where

- ζ = Proportionality coefficient

The complete model consists in coupling the electromagnetic problem equation 3.77-equation 3.83 with the thermal problem equation 3.84, equation 3.85 or equation 3.86, where T depends only on the spatial coordinates r , θ and on the time t .

This model includes two kinds of nonlinearities: the first due to the heat source term in the heat equation 3.81 and the second due to the dependence of physical properties of the non-conducting materials on the temperature and possibly on the magnetic field.

3.5 Depth of Penetration

Penetration Depth is a measure of how deep light or any electromagnetic radiation can penetrate into a material. A number of things can influence penetration depth, including properties of the material itself, the intensity and frequency of the radiation, and various environmental factors. It has been defined as the depth at which the intensity of the radiation inside the material falls to $1/e$ (about 37%) of its original value at (or more properly, just beneath) the surface.

When electromagnetic radiation is incident on the surface of a material, it may be (partly) reflected from that surface and there will be a field containing energy transmitted into the material. This electromagnetic field interacts with the atoms and electrons inside the material. Depending on the nature of the material, the electromagnetic field might travel very far into the material, or may die out very quickly. For a given material, penetration depth will generally be a function of wavelength. The depth of penetration, δ , is defined as the depth, which has been attenuated to $\frac{1}{e}$ or approximately 37% of the original value.

The amplitude of the wave decreases by a factor $e^{-\alpha x}$, where α is attenuation constant, it is apparent that a distance x which makes $\alpha x = 1$, the amplitude is only $\frac{1}{e}$ times its value at $x = 0$. This distance is equal to δ , the depth of penetration,

$$\alpha x = 1 \text{ or } \alpha \delta = 1, \delta = \frac{1}{\alpha}$$

$$\delta = \frac{1}{\alpha} = \frac{1}{\omega \sqrt{\frac{\mu \epsilon}{2} \left(\sqrt{1 + \frac{\sigma^2}{\omega^2 \epsilon^2}} - 1 \right)}} \quad (3.87)$$

For a conducting material $\frac{\sigma}{\omega \epsilon} \gg 1$, so

$$\delta = \frac{1}{\alpha} = \sqrt{\frac{2}{\omega \mu \sigma}} = \sqrt{\frac{1}{\pi f \mu \sigma}} \quad (3.88)$$

3.6 Wave Reflection and Transmission

When wave propagating in a uniform medium encounters an interface with a different medium, a portion of the wave is reflected from the interface while the remainder of the wave is transmitted. The reflected and transmitted waves can be determined by enforcing the fundamental electromagnetic field boundary conditions at the media interface.

Given a z-directed, x-polarized uniform plane wave incident on a planar media interface located on the x-y plane, the phaser fields associated with the incident, reflected and transmitted fields may be written as:

Incident wave fields

$$\begin{aligned} E_x^i &= E_{x0}e^{-\gamma z} \\ H_y^i &= \frac{E_{x0}e^{-\gamma z}}{\eta_1} \end{aligned} \quad (3.89)$$

Reflected wave fields

$$\begin{aligned} E_x^r &= \Gamma E_{x0}e^{-\gamma z} \\ H_y^r &= \Gamma \frac{E_{x0}e^{-\gamma z}}{\eta_1} \end{aligned} \quad (3.90)$$

Transmitted wave fields

$$\begin{aligned} E_x^t &= \Upsilon E_{x0}e^{-\gamma z} \\ H_y^t &= \Upsilon \frac{E_{x0}e^{-\gamma z}}{\eta_2} \end{aligned} \quad (3.91)$$

Where

- Γ = Reflection coefficient
- Υ = Transmission coefficient
- η_1 = Reflected intrinsic impedance
- η_2 = Transmission intrinsic impedance

Enforcement of the boundary conditions (continuous tangential electric field and continuous tangential magnetic field) yields

$$E_x^i + E_x^r + E_x^t \text{ at } z = 0 \rightarrow 1 + \Gamma = \Upsilon$$

$$H_x^i + H_x^r + H_x^t \text{ at } z = 0 \rightarrow \frac{1-\Gamma}{\eta_1} = \frac{\Upsilon}{\eta_2}$$

Solving these two equations for the reflection and transmission coefficients gives

$$\text{Reflection coefficients } \Gamma = \frac{\eta_2 - \eta_1}{\eta_2 + \eta_1}$$

$$\text{Transmission coefficient } \Upsilon = \frac{2\eta_2}{\eta_2 + \eta_1}$$

The different condition of intrinsic impedance has been represented as per material characteristics shown in Table 3.1.

Table 3.1: Effects of Intrinsic Impedance

Case	Intrinsic impedance	Reflection Coefficient	Transmission Coefficient	Remark
I	$\eta_1 = \eta_2$	$\Gamma = 0$	$\Upsilon = 1$	Total transmission, No reflection
II	$\eta_1 = 0$	$\Gamma = 1$	$\Upsilon = 2$	Total reflection without inversion of E
III	$\eta_2 = 0$	$\Gamma = -1$	$\Upsilon = 0$	Total reflection with inversion of E
IV	$\eta_2 > \eta_1$	$0 < \Gamma < 1$	$1 < \Upsilon < 2$	
V	$\eta_2 > \eta_1$	$0 < \Gamma < 1$	$0 < \Upsilon < 1$	

Table 3.2: Characteristics of Materials

Sr. No.	Types of Material	Conductivity σ s/m	Permittivity ϵ F/m	Permeability μ H/m
1	Water	2×10^{-4}	80	0.999991
2	Aluminum	3.54×10^7	1	1.000021
3	Copper	5.80×10^7	1	0.999991
4	Stainless steel	10^6	1	1
5	Lemon / Orange	4	80	1
6	Tomatoes	2.5	80	1

3.7 Operating Parameters

Values of electrical conductivity, permittivity and permeability employed for calculation are presented in Table 3.2 and operating parameters are listed in Table 3.3. The system under consideration includes a right cylindrical conductor for steel and sphere for lemon load in the direction of O_z and O_θ respectively, which are surrounded by a multi turn cylindrical induction coil.

Therefore, it is realistic to assume that the coil is always at room temperature. Assume a total voltage of the coil is $V_{coil} = 200V$ with a frequency of 10 Hz to 1000 K Hz. The driving current density in the IDH coil is calculated by $J_0 = \sigma_{co} V_{coil} / (2\pi R_{co} N)$,

Where

- V_{coil} = Total voltage of the coil
- R_{co} = The mean value of the coil radius
- N = The number of coil turns

For the magnetic permeability (μ), assume that it is everywhere the constant value of free space $\mu = \mu_r \mu_0 \simeq \mu_0$ (i.e. $\mu_r \simeq 1$).

Table 3.3: Operating Parameters

Sr. No.	Description (Units in mm)	Symbol	Value For steel	Value For lemon
1	Work-piece radius	r_w	55	35
2	Work-piece height	h_w	40	-
3	Coil inner radius	r_{co}	85	85
4	Coil width	L_{co}	20	20
5	Coil wall thickness	l_{co}	5	5
6	Height of coil turns	h_{co}	40	40
7	Distance between coil turn	d_{co}	2.5	2.5

Where

μ_r = The relative magnetic permeability

The quantity $\delta_w = (2/\mu_w\sigma_w\omega)^{1/2}$ has the dimension of length and is called the skin depth (or penetration depth). It is a measure of the field penetration depth into the materials. In our calculation the corresponding skin depth of the steel and lemon work-pieces are $\delta_w = 2.5mm$ and $\delta_w = 1.5mm$ respectively.

It should be mentioned here that since IDH is a very complicated process, one can not expect accurate simulation of the whole chain of coupled phenomena - electromagnetic, thermal, mechanical, hydrodynamic and metallurgical - during a heating process. The most important and controllable process is electromagnetic which is analyzed here.

3.8 Numerical Solution

The standard finite element method has been adopted for the discrimination of equation 3.53, equation 3.54, equation 3.77 and equation 3.78. Finite differences in time and standard finite elements in space have been used to solve the heat equation. The mesh used for the thermal problem is same as the part of the mesh used for the electromagnetic problem inside the materials. It is worth noticing that the skin effect requires a particularly refined mesh close to the boundary of the materials. On the other hand, coarse mesh size would result an inaccurate solution of heat equation. Therefore, a reasonable compromise has to be found.

The electromagnetic problem is solve by stationary time, while the heat equation gives

rise to an evaluative problem. Due to the different time scale of the two phenomena, it is assumed that the solution of the electromagnetic problem is valid on a time interval and the physical properties of the work-pieces do not change much, due to the increases in temperature resulting from the Joule / Rubbing effect. Then these results are used to compute the source term to be plugged into the heat equation. The evaluative heat equations have been solved using finite difference on the same time interval. The new values of the temperature field thus obtained have been used to update the values of the physical coefficient of the work-pieces. This will allow us to proceed to another computation of magnetic potential, followed by the computations of the temperature field and so on.

A numerical simulation code has been developed based on the above model. It can be dealt with any IDH system having an axis symmetric geometry. Only sinusoidal voltage is allowed, but the restriction on the shape of the voltage does not have a big effect from the energetic point of view. The possibility of having several electric current generators, characterized by different frequency, voltage amplitudes and possibly different phases, has been taken into account.

3.9 Simulation Results

Attenuation constant, phase constant and propagation constant for conducting material (stainless steel) simulation results are shown in Figure 3.1, Figure 3.2 and Figure 3.3, respectively. Figure 3.4 shows skin depth for conducting material. Velocity of propagation and intrinsic impedance for stainless steel are shown in Figure 3.5 and Figure 3.6, respectively. The velocity of propagation and intrinsic impedance for conducting material is small and a reactive component with impedance angle of 45° determined from equation 3.44 and simulation shown in Figure 3.7. Figure 3.8, Figure 3.9, Figure 3.10 and Figure 3.11 show simulation of loss tangent, electric field intensity, magnetic field intensity and power density for conducting material, respectively.

Attenuation constant, phase constant and propagation constant for non-conducting material (lemon/orange) simulation results are shown in Figure 3.12, Figure 3.13 and Figure 3.14, respectively. Figure 3.15 shows skin depth for non-conducting material. Velocity of propagation and intrinsic impedance for lemon/orange are shown in Figure 3.16

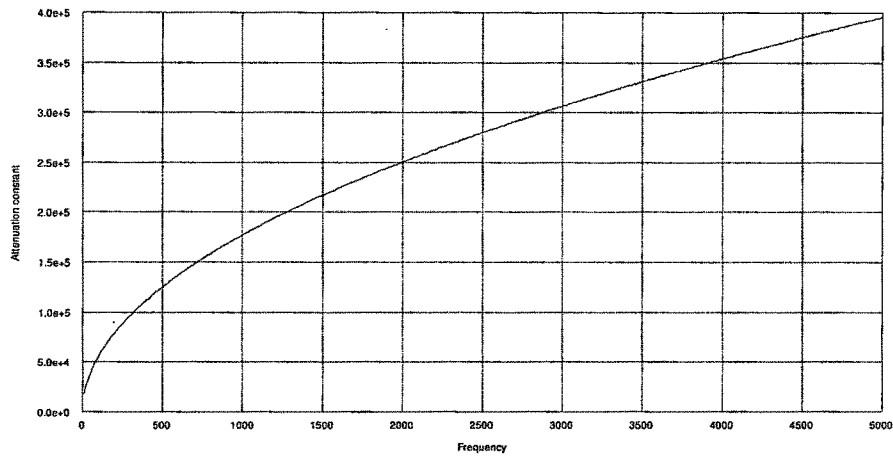


Figure 3.1: Attenuation Constant for Stainless Steel

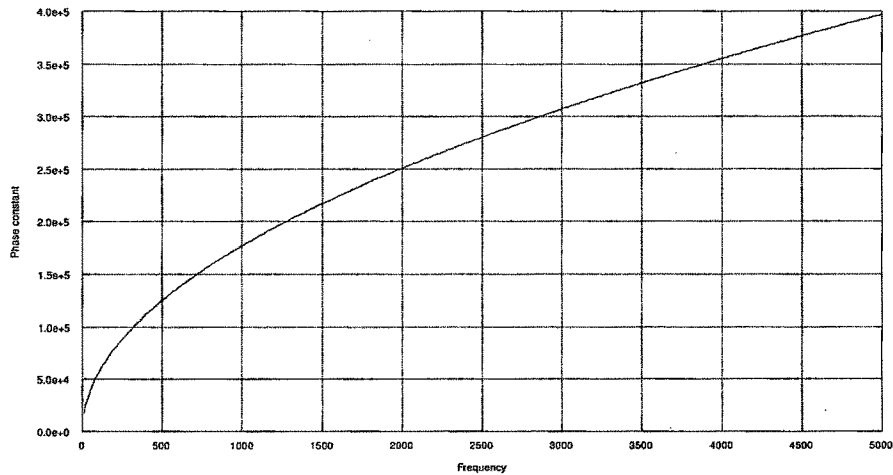


Figure 3.2: Phase Constant for Stainless Steel

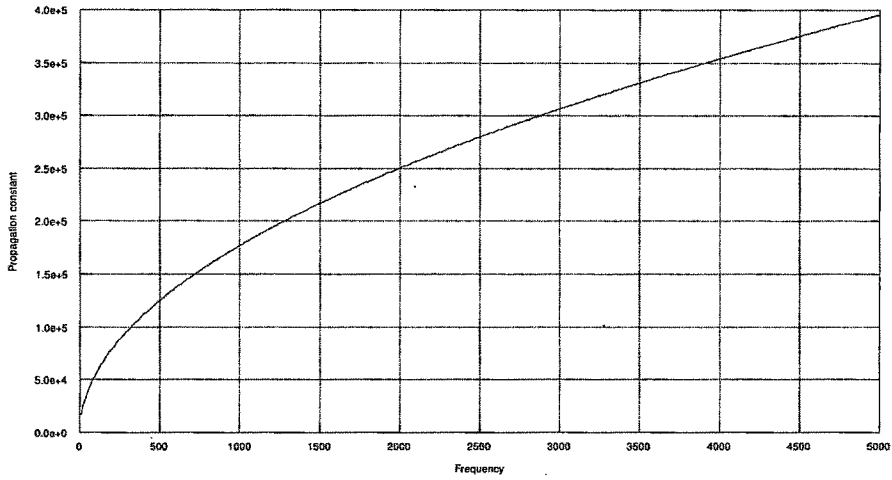


Figure 3.3: Propagation Constant for Stainless Steel

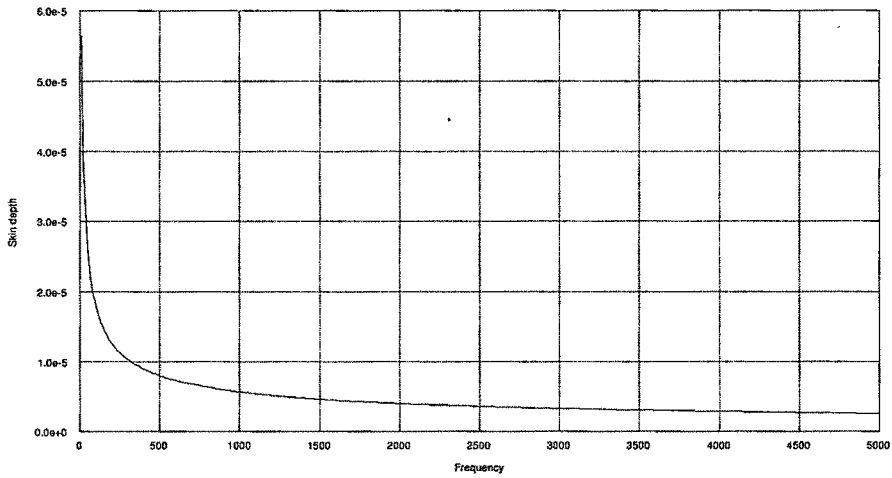


Figure 3.4: Skin Depth for Stainless Steel

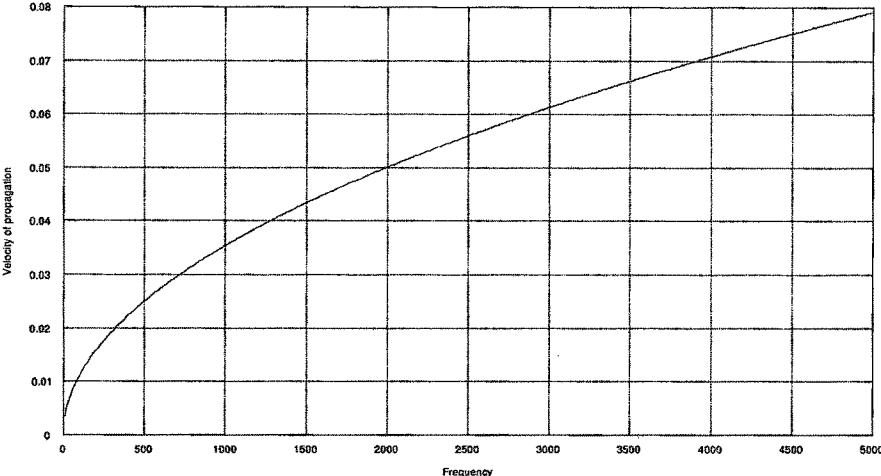


Figure 3.5: Velocity of Propagation for Stainless Steel

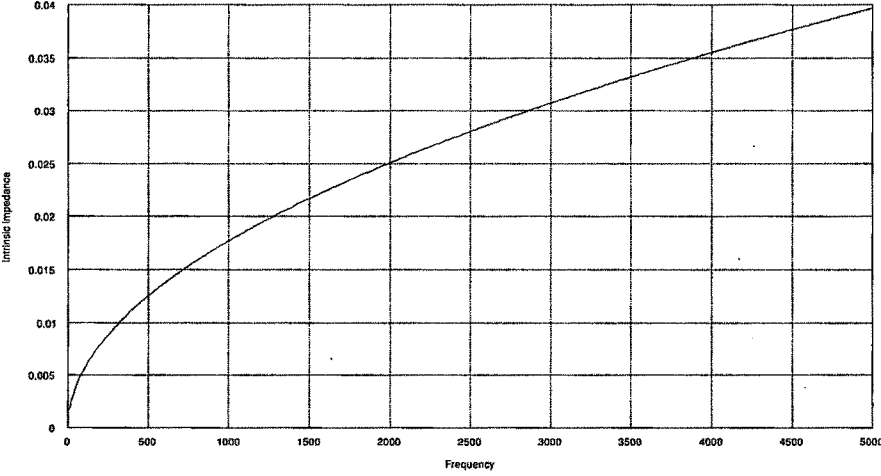


Figure 3.6: Intrinsic Impedance for Stainless Steel

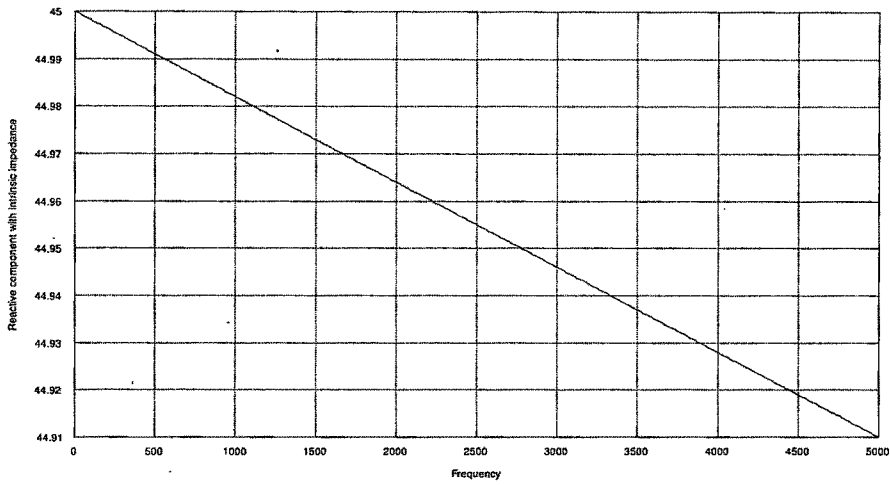


Figure 3.7: Reactive Component With Intrinsic Impedance for Stainless Steel

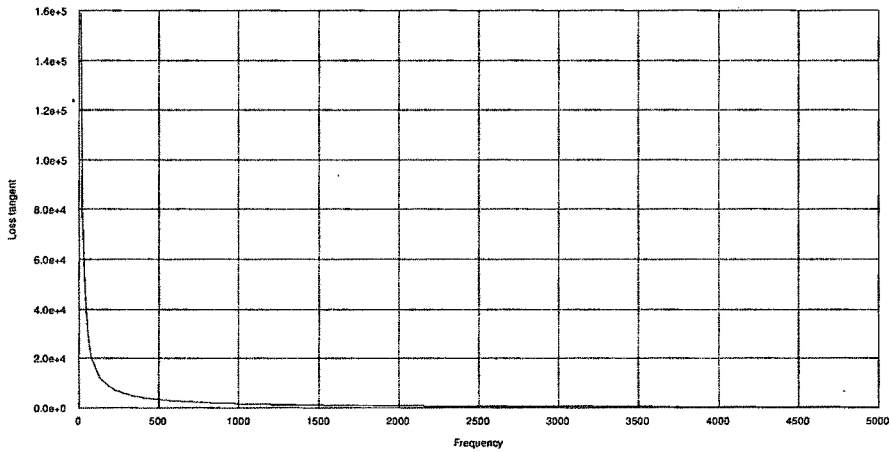


Figure 3.8: Loss Tangent for Stainless Steel

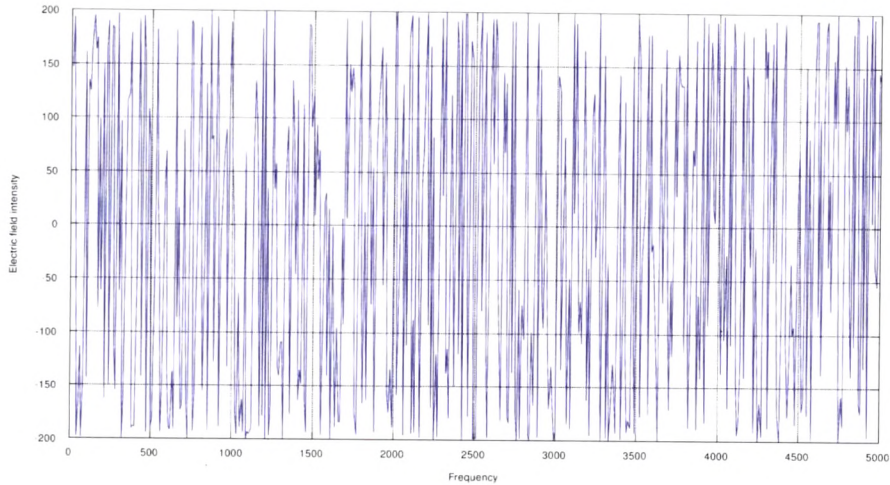


Figure 3.9: Electric Field Intensity for Stainless Steel

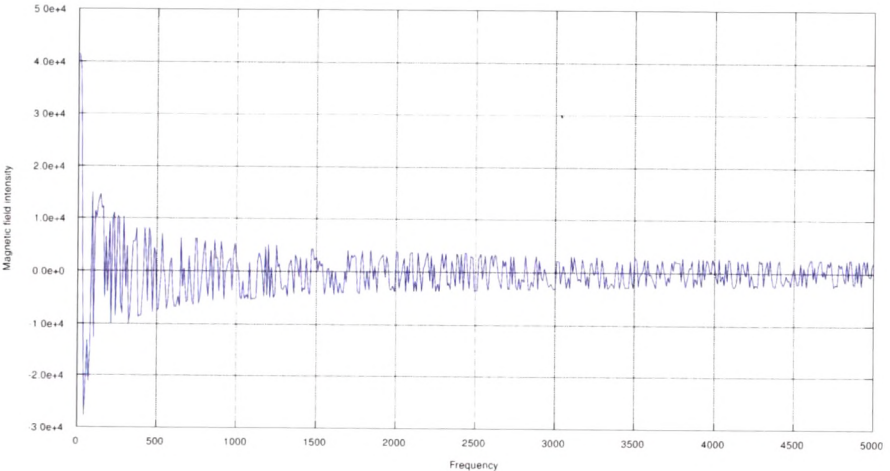


Figure 3.10: Magnetic Field Intensity for Stainless Steel

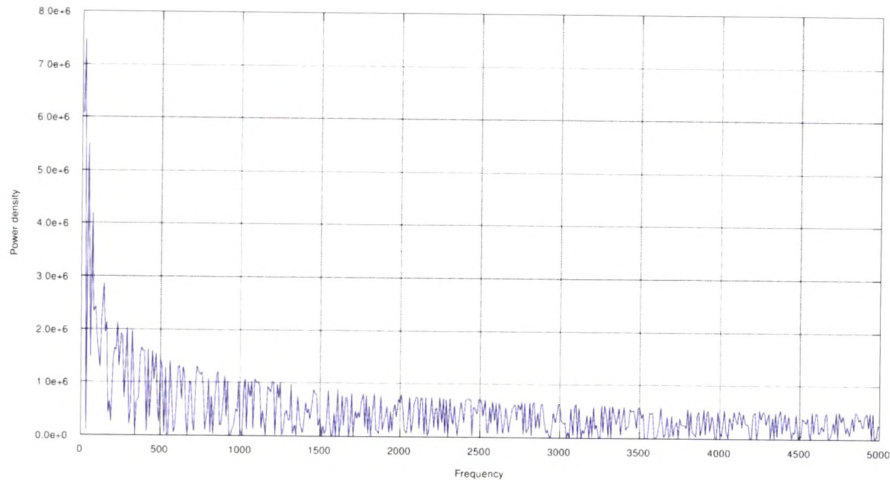


Figure 3.11: Power Density for Stainless Steel

and Figure 3.17, respectively. The velocity of propagation and intrinsic impedance for non-conducting material is remaining constant and a small reactive component with intrinsic impedance determined from equation 3.68 and simulation shown in Figure 3.18. Figure 3.19, Figure 3.20, Figure 3.21 and Figure 3.22 show simulation of loss tangent, electric field intensity, magnetic field intensity and power density for non-conducting material, respectively.

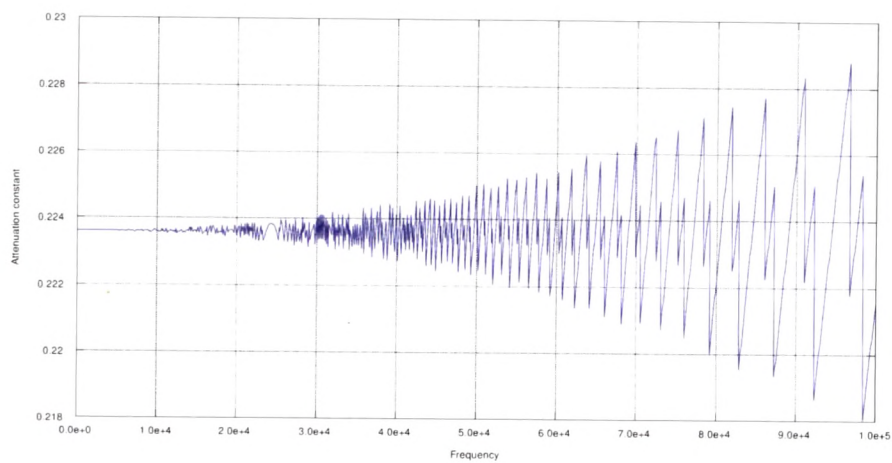


Figure 3.12: Attenuation Constant for Lemon / Orange

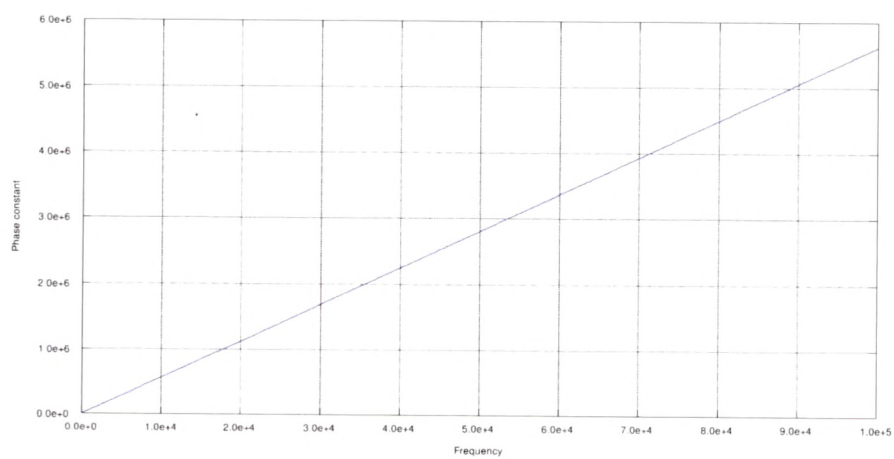


Figure 3.13: Phase Constant for Lemon / Orange

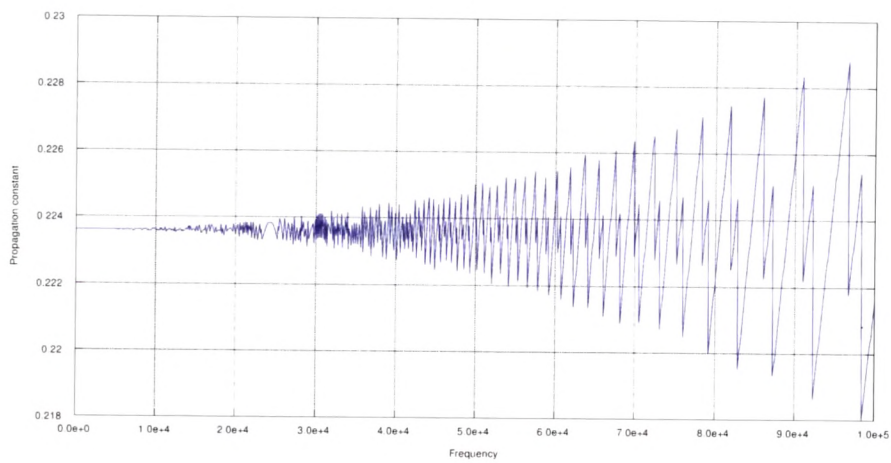


Figure 3.14: Propagation Constant for Lemon / Orange

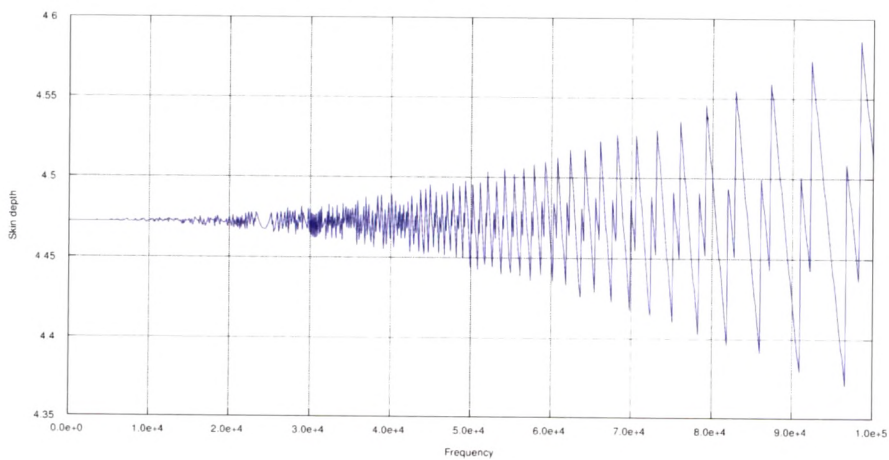


Figure 3.15: Skin Depth for Lemon / Orange

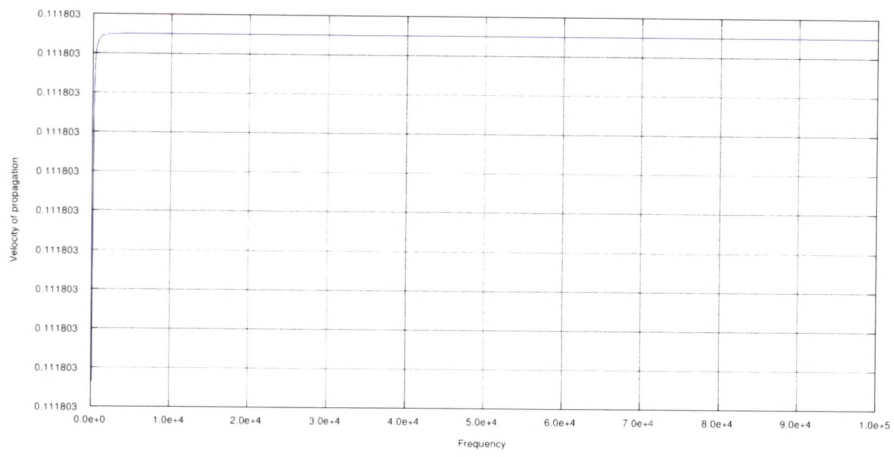


Figure 3.16: Velocity of Propagation for Lemon / Orange

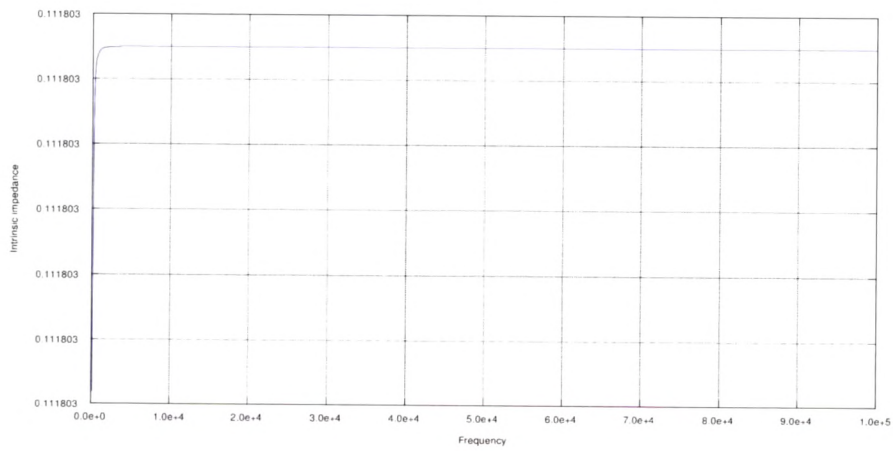


Figure 3.17: Intrinsic Impedance for Lemon / Orange

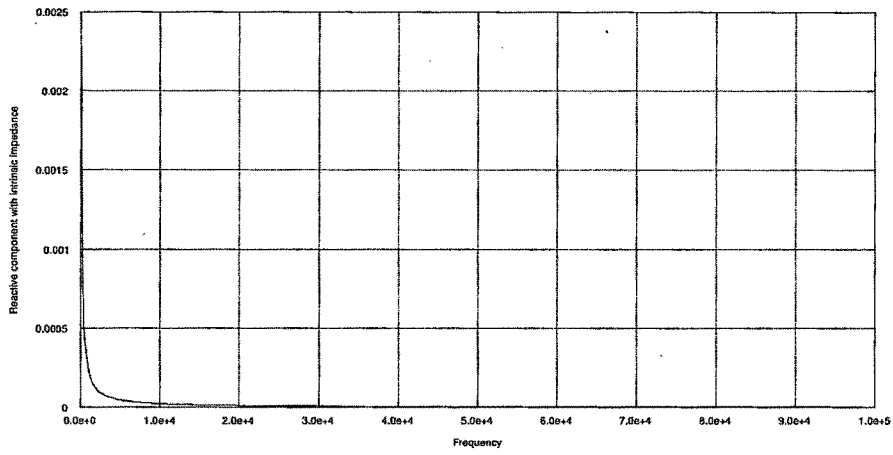


Figure 3.18: Reactive Component With Intrinsic Impedance for Lemon / Orange

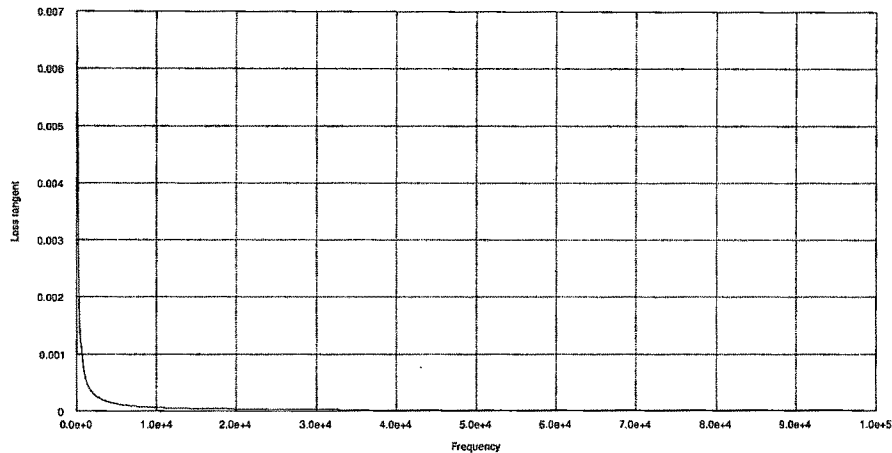


Figure 3.19: Loss Tangent for Lemon / Orange

The finite element mesh analysis is shown in Figure 3.23 for non-conducting material (lemon). Figure 3.24, Figure 3.25, and Figure 3.26 show different temperature analysis, Skin depth analysis using finite element method (FEM), respectively. The displacement current are shown in Figure 3.27 and Figure 3.28 for non-conducting material at different frequency using FEM. Figure 3.29, Figure 3.30, Figure 3.31, and Figure 3.32 show magnetic field density and magnetic field intensity for lemon at different frequency using FEM, respectively.

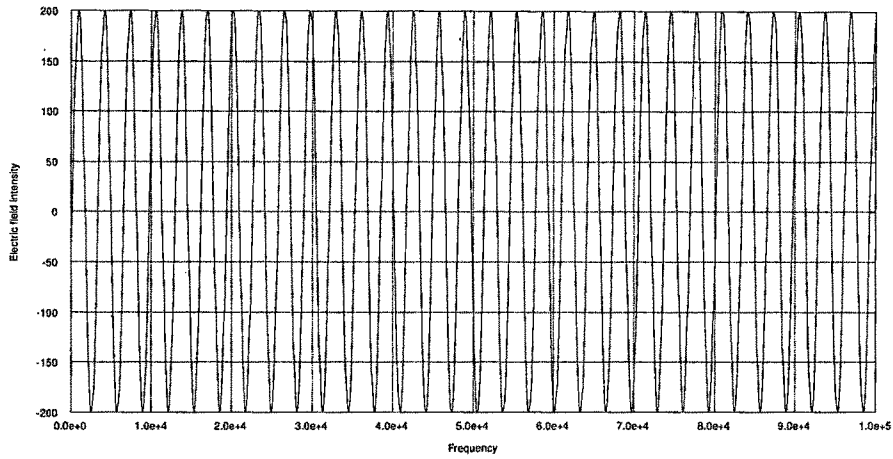


Figure 3.20: Electric Field Intensity for Lemon / Orange

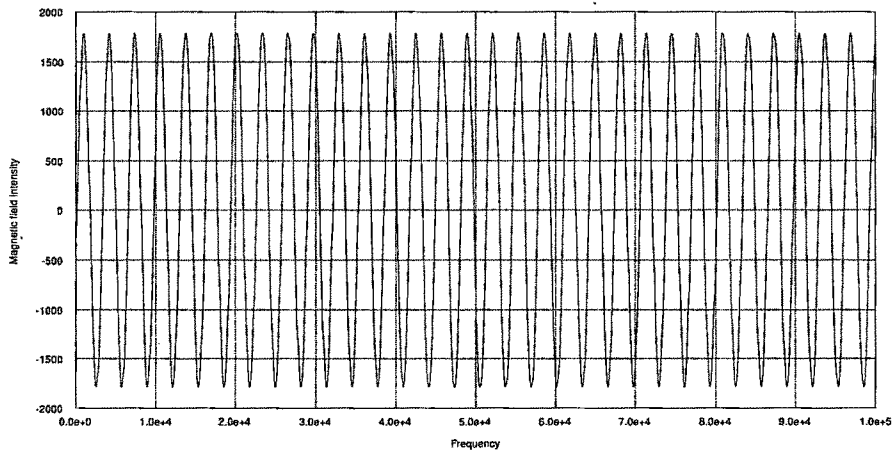


Figure 3.21: Magnetic Field Intensity for Lemon / Orange

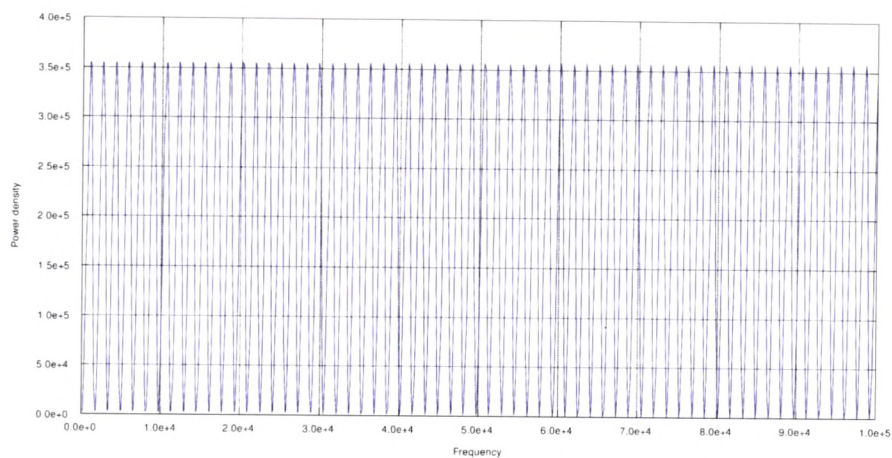


Figure 3.22: Power Density for Lemon / Orange

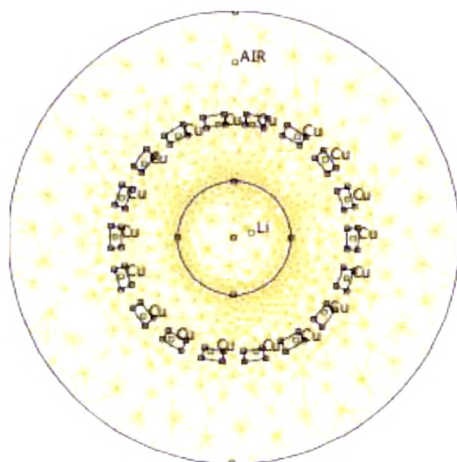


Figure 3.23: Mesh Analysis for Lemon

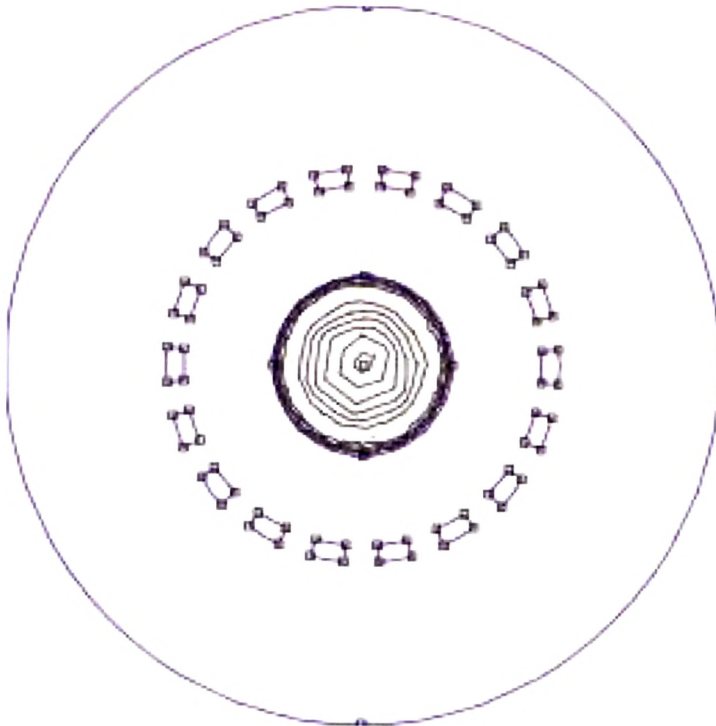


Figure 3.24: Temperature Analysis Using FEM

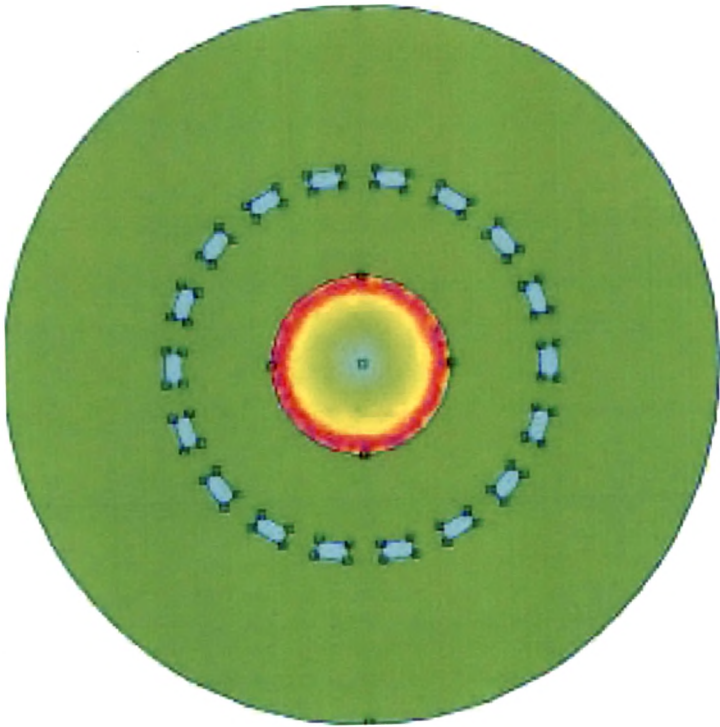


Figure 3.25: Skin Depth Analysis Using FEM

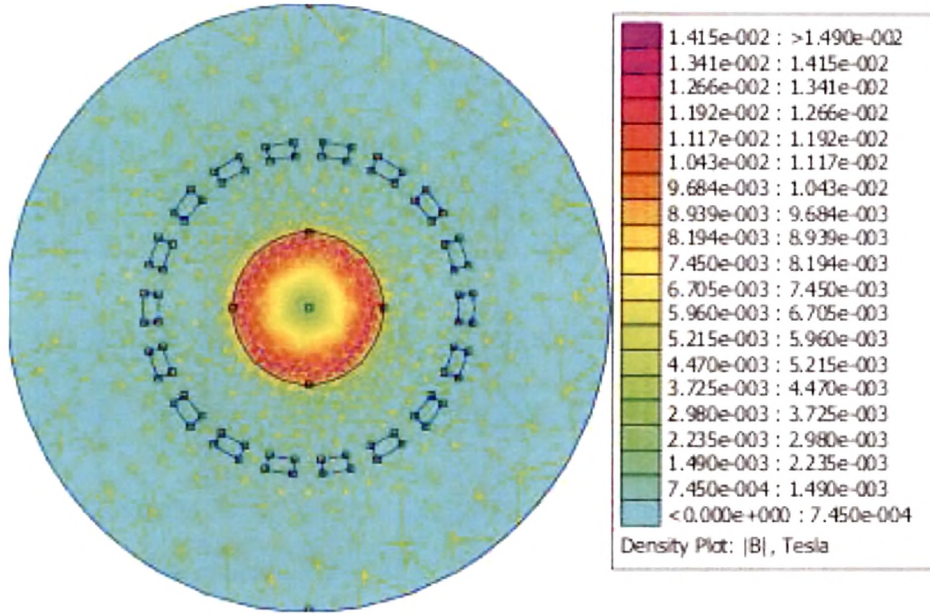


Figure 3.26: Temperature and Skin Depth Analysis With Density Using FEM for Lemon

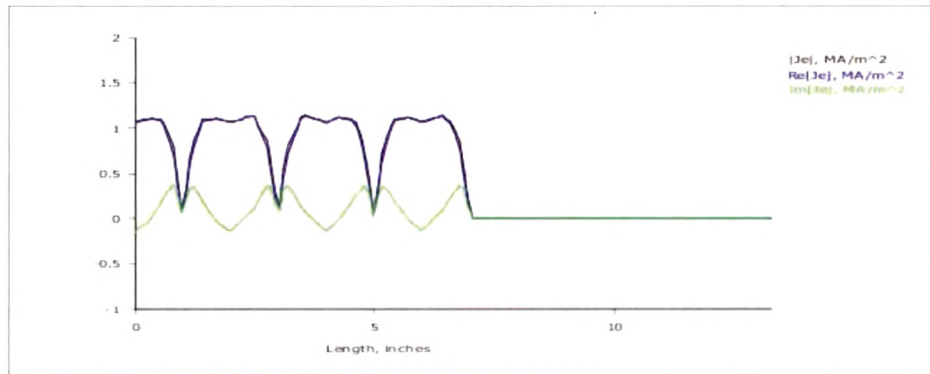


Figure 3.27: Displacement Current for Lemon Using FEM at 10 MHz

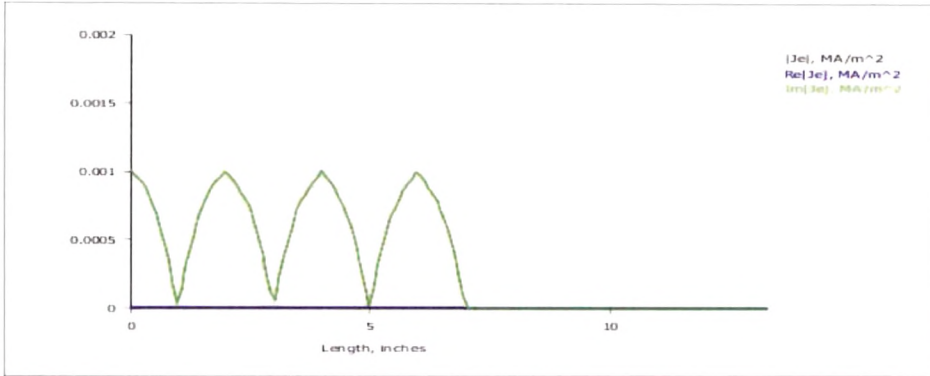


Figure 3.28: Displacement Current for Lemon Using FEM at 1KHz

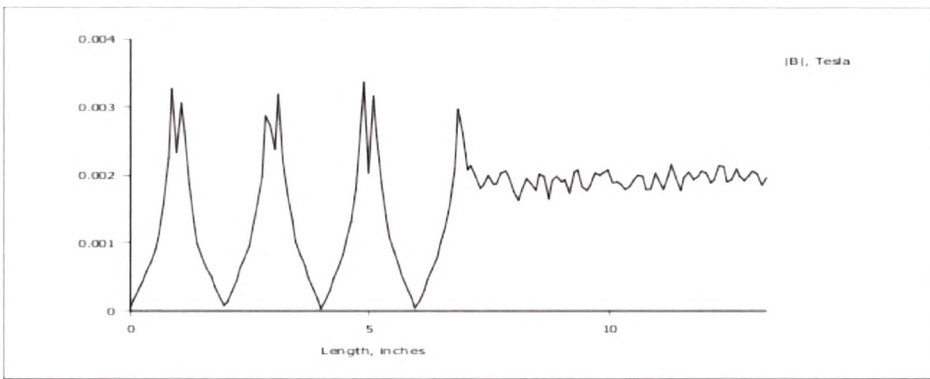


Figure 3.29: Magnetic Field Density for Lemon Using FEM at 10MHZ

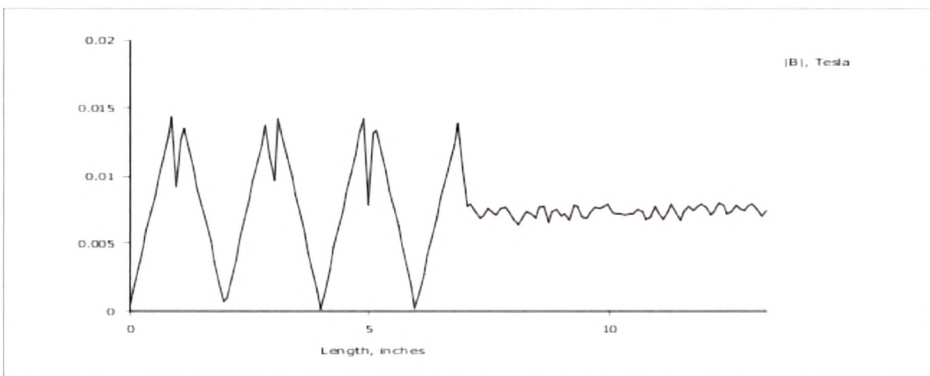


Figure 3.30: Magnetic Field Density for Lemon Using FEM at 1KHz

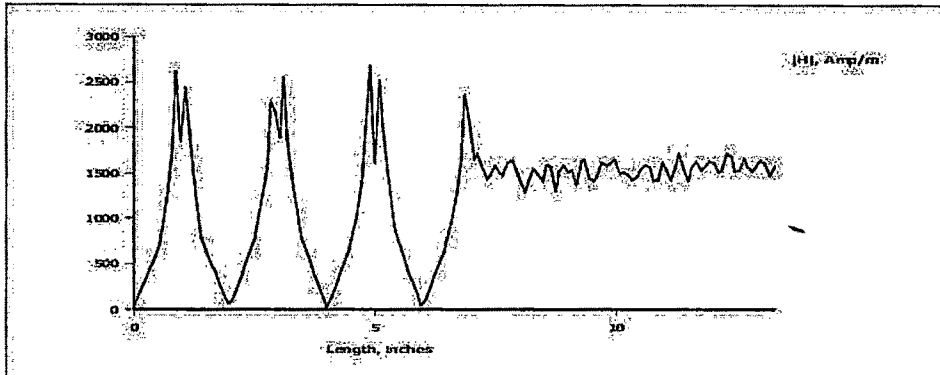


Figure 3.31: Magnetic Field Intensity for Lemon Using FEM at 10MHz

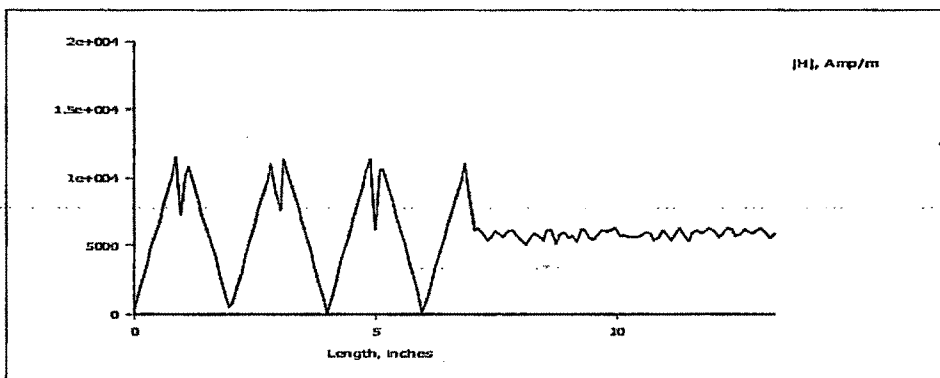


Figure 3.32: Magnetic Field Intensity for Lemon Using FEM at 1KHz

3.10 Conclusions

A mathematical model for obtaining a reflection coefficient, transmission coefficient and electromagnetic wave properties for the work-piece contribution to the impedance of a given IDH system has been derived. This is intended to assess how work-piece is linked to the excitation loop, thus in order to find out conditions where the eddy current or displacement current occurrence is enhanced. Empirical rules already known by IDH practitioners have been proved and the finding can be extrapolated to design new possibilities. The proposed approach has been validated using MATLAB and FEM software.

The main finding of this chapter reveals following:

1. As frequency increases, the current becomes concentrated along the outer surface of the object.
2. The electromagnetic shield may be necessary to prevent waves from radiating out of the shielded volume or to prevent waves from penetrating into the shielded volume.
3. Attenuation constant, phase constant and propagation constant increases with increase in frequency in conducting material and non-conducting material.
4. Intrinsic impedance increases with increase in frequency in conducting material and is remaining constant with increase in frequency for non-conducting material.
5. Velocity of propagation and intrinsic impedance of conducting material exponentially increases with increase in frequency and reactive component of conducting material remains constant at 45° .
6. Velocity of propagation and intrinsic impedance of non-conducting material remains constant with increase in frequency and reactive component of non-conducting material is small.